Desalination and Water Treatment
www.deswater.com

doi: 10.5004/dwt.2022.28525

261 (2022) 308–321
June

Removal of tetracycline antibiotic from aqueous solution using biosorbent

Müslün Sara Tunç, Özge Hanay*

Department of Environmental Engineering, Faculty of Engineering, Firat University, Elazig 23119, Turkey, Tel. +90 533 7201610; emails: ohanay@firat.edu.tr (Ö. Hanay), saratunc@firat.edu.tr (M.S. Tunç)

Received 1 December 2021; Accepted 20 April 2022

ABSTRACT

As the accumulation of antibiotics has led to increasingly serious environmental pollution problems, many studies have revealed that the adsorption method can be used to efficiently and easily remove residual antibiotics in water with low cost and high efficiency. Chitin being a biosorbent has recently received attention as a new type of adsorption material. The tetracycline (TC) adsorption by chitin was studied through characterization and analysis of chitin and as a function of solution pH, adsorbent dosage, temperature and initial TC concentration. The highest TC adsorption capacity was determined as 7.08 mg/g for initial TC concentration of 80 mg/L at pH 7 and 55°C. The adsorption process obeyed the pseudo-second-order kinetic model and Freundlich and Dubinin–Radushkevich adsorption isotherm models. TC adsorption onto chitin was also endothermic and spontaneous. The adsorption of TC by chitin was primarily controlled by physical adsorption and chemical adsorption including pore filling, hydrogen bonding and weak electrostatic interaction.

Keywords: Adsorption kinetics; Biosorbent; Chitin; Tetracycline; Thermodynamic

1. Introduction

Antibiotics in human and animal therapy and aquaculture have been increasingly used worldwide in the recent years either to prevent or treat microbial infections [1,2]. The common usage of antibiotics has become a serious problem due to negative influences such as acute and chronic toxicity, influence on aquatic organisms, obliteration of native microbial population, and enhancement of antibiotic-resistant genes [3]. Tetracycline (TC) contaminates the soil and surface and groundwater through leaching or runoff when released into the environment [4]. The concentration of TC could reach to μg/L and mg/L in natural water and in medical wastewater, respectively [5,6]. The toxicological effects of TC and the environmental behavior in aquatic environment have been evaluated in previous studies. Jiao et al. [7] reported that the toxicity of TC photoinhibition of *Vibrio fischeri* and photodegradation products were more toxic than the parent compounds [7]. In another study, it was determined that a binary mixture of TC and 7-aminocephalosporin caused antagonistic toxicity on green algae *Selenastrum capricornutum* [8]. The presence of TC in water at high concentrations may cause gastrointestinal irritation, vomiting, diarrhea, and renal failure. Because TC is absorbed into bones, it may form a stable calcium complex in bone, causing a decrease in bone growth rate. TC has also toxic effects on the developing fetus [4].

TCs are amphoteric owing to the entity of dimethylamino group, phenolic diketone group and tricarbonylamide group [1]. Since they are not completely metabolized by humans and animals, the majority are excreted via urine and feces as unchanged parent compounds [2,3]. Due to the antibacterial characteristics, it is difficult to remove TC completely through biological treatment [9,10]. Several researchers investigated the removal of TC antibiotics by

* Corresponding author.

various treatment technologies such as ozonation [11], photo-Fenton process [12], photo-electro-Fenton [13], electrocoagulation [14] and adsorption [15]. However, most of them are expensive due to their high maintenance and process cost [16].

In comparison to these techniques, adsorption is considered as an eminent treatment approach to deal with the containing-TC wastewater owing to its easy operation, low cost and high removal efficiency and various adsorbents such as activated carbon [10,17], biochar [18,19], single- and multi-walled carbon nanotubes [20], graphene oxide [3], goethite [21], microscale zero-valent iron [22], kaolinite [1], palygorskite [23], modified magnetic bentonite [24], N-doped hollow carbon [25] have been used. Moreover, the adsorption method becomes an attractive alternative treatment when the adsorbent such as chitin, chitosan, clays, zeolites, peat soils, fly ashes and coals is low-cost and readily available [26,27]. Among them, chitin has attracted considerable attention for removing of hazardous contaminants from water due to its sorption capacity and more eco-friendly characteristics [28–30].

Chitin is a biopolymer and a non-toxic polysaccharide which makes it biodegradable [27]. It is also the second most abundant natural polymer in the world [31] which is generally attained from wastes consisting of fundamentally shells of crab, shrimp, prawn and krill in the seafood processing industries [32]. Research into the removal and adsorption mechanism for antibiotic by chitin is rarely involved at present. Żółtowska-Aksamitowska et al. [33] studied the use of chitin modified with kraft lignin as an effective sorbent of ibuprofen and acetaminophen. The surface modification of chitin using kraft lignin results in a material with a surface rich in functional groups, making it a more effective sorbent of hydrophobic impurities in comparison with the precursors.

Based on the above background, we explored the removal performance and adsorption behavior and mechanism of chitin for TC for the first time. In this study, chitin was characterized and analyzed by scanning electron microscopy (SEM), Fourier-transform infrared spectroscopy (FTIR) and Brunauer–Emmett–Teller (BET) to explore the change in the material before and after adsorption process. At the same time, the influence of parameters including temperature, solution pH, chitin dosage and initial TC concentration on the adsorption performance was studied. The adsorption mechanism was analyzed through kinetics and isotherm model fitting, combined with characterization analysis before and after adsorption.

2. Materials and methods

2.1. Chemicals

Tetracycline hydrochloride, $C_{22}H_{24}N_2O_8{\cdot}HCI$, was purchased from Applichem and used without further purification. The structure is given in Fig. 1a. Acetonitrile with HPLC grade was purchased from Merck. Ethanol, H_2SO_4 and NaOH were purchased from Sigma-Aldrich.

2.2. Adsorbent

Chitin was from crushed crab shells and purchased from Sigma Chemicals Co. The molecular formula of chitin is $(C_8H_{13}O_5N)_n$ and its molecular structure is shown in Fig. 1b. It was sieved to separate the material into different particle size ranges before using in the experiments. The particle sizes of 297–841 μm (in the size of −20 + 50 mesh) could be chosen for adsorption experiments.

2.3. Adsorption studies

The TC stock solution of 200 mg/L was daily prepared to avoid degradation caused by oxygen and light. The concentrations of prepared TC solutions varied in the range of 10 and 80 mg/L. The initial pH of TC solutions was adjusted by diluted H_2SO_4 or NaOH solution prior to addition of chitin. All working solutions were prepared with distilled water.

The batch experiments were conducted using Erlenmeyer flasks of 250 mL containing 100 mL of TC solutions in an orbital shaker incubator (Gallenkamp) at 150 rpm. 5 mL samples were withdrawn at particular time intervals after adding chitin for TC analysis. The samples were centrifuged at 1,500 rpm for 2 min and then the supernatant was filtered through 0.22 μm membrane syringe filter.

The effects of some variables including solution pH, initial TC concentration, chitin amount and temperature on adsorption process were examined. To detect the influence of solution pH on TC adsorption onto chitin, solution pH was investigated by varying between pH 3 and pH 9. The

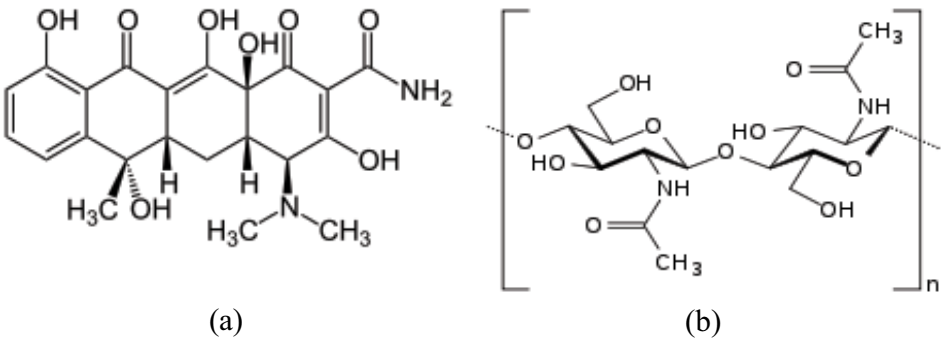

Fig. 1. Molecular structure of tetracycline (a) and chitin (b).

influence of chitin amount was evaluated by varying the amount of chitin in the range of 1 and 10 g/L while the effect of temperature on TC adsorption onto chitin was conducted at 25°C, 40°C and 55°C. The initial TC concentration ranged from 10 to 80 mg/L. All experiments were undertaken in duplicate and the average results were considered.

2.4. Removal efficiency and adsorption capacity

TC removal efficiency was calculated according to Eq. (1):

$$\text{TC removal}\left(\%\right)=\frac{\left(C_0-C_t\right)}{C_0}\times 100 \tag{1}$$

where C_0 is the initial concentration of TC in liquid (mg/L) and C_t is the concentration of TC in liquid at any time (mg/L).

The adsorbed TC amount at equilibrium per unit mass of chitin, q_e (mg/g), was obtained from Eq. (2) whereas the adsorbed TC amount at any time per unit mass of chitin, q_t (mg/g), was determined according to Eq. (3):

$$q_e=\frac{\left(C_0-C_e\right)V}{m} \tag{2}$$

$$q_t=\frac{\left(C_0-C_t\right)V}{m} \tag{3}$$

where C_e is the equilibrium concentration of TC in liquid (mg/L), V is the volume of TC solution (L), and m is the amount of chitin (g).

2.5. Methods of analysis

The concentration of TC in the filtrate was determined by using high-performance liquid chromatography (HPLC, Shimadzu SIL-20AHT) using an AllureBiPh column (5 μm, 150 mm × 4.6 mm). The mixture of 20 mM ammonium dihydrogen-phosphate (pH 2.5) and acetonitrile (20/80, v/v) was used as mobile phase. The flow rate was set at 1.2 mL/min and injection volume of 100 μL was used. TC was analyzed by a diode array detector at 269 nm. The retention time was determined as 4 min. The solution pH was determined using a pH meter (Orion 3 STAR).

The surface structure of chitin before and after TC adsorption was determined by scanning electron microscopy (Jeol-JSM-7001F). The FTIR spectra of chitin were recorded with a FTIR spectrometer (ATI Unicam Mattson 1000) by averaging 16 scans in the range of 400–4,000 cm^{-1}. The BET surface area was performed using nitrogen adsorption method by an Autosorb IQ2 Surface Area Analyzer.

2.6. Adsorption isotherms

Adsorption isotherm study was conducted on Langmuir, Freundlich and Dubinin–Radushkevich isotherms. The Langmuir equation based on monolayer adsorption onto homogeneous surface of adsorbent is expressed as [34]:

$$q_e=\frac{q_{\max}K_LC_e}{1+K_LC_e} \tag{4}$$

where K_L is the Langmuir constant related to the adsorption energy (L/mg) and $q_{\max}$ is the maximum adsorption capacity (mg/g). The linear form of Eq. (4) becomes as follows:

$$\frac{C_e}{q_e}=\frac{C_e}{q_{\max}}+\frac{1}{K_Lq_{\max}} \tag{5}$$

Langmuir parameters can also be utilized to determine whether the adsorption is favorable. To define this, separation factor (R_L), a significant parameter in Langmuir isotherm, must be determined. It is defined by Eq. (6) [35]:

$$R_L=\frac{1}{1+K_LC_0} \tag{6}$$

where R_L value demonstrates the characteristic of adsorption process to be irreversible ($R_L = 0$), favorable ($0 < R_L < 1$), linear ($R_L = 1$) or unfavorable ($R_L > 1$) [35].

The Freundlich model based on the multilayer sorption on heterogeneous surfaces is an empirical equation, assuming that binding sites are not equal and/or independent. It is defined by the following equation [36]:

$$q_e=K_FC_e^{1/n} \tag{7}$$

where K_F and n are Freundlich constants which indicate adsorption capacity and adsorption intensity, respectively. The linearized form of Eq. (7) is:

$$\ln q_e=\ln K_F+\frac{1}{n}\ln C_e \tag{8}$$

Dubinin–Radushkevich isotherm model is generally employed to describe the mechanism of adsorption and designate the nature of adsorption as physical or chemical based on the free mean sorption energy [37]. Dubinin–Radushkevich isotherm model [38] is represented as:

$$q_e=q_{\text{DR}}e^{-K_{\text{DR}}\varepsilon^2} \tag{9}$$

where q_e is the mole amount of TC adsorbed on per unit weight of chitin (mol/g), q_{DR} is the theoretical isotherm saturation capacity (mol/g), K_{DR} is the isotherm constant related to the adsorption energy (mol^2/J^2), and ε is the Polanyi potential related to equilibrium, which can be calculated by Eq. (10):

$$\varepsilon=RT\ln\left(1+\frac{1}{C_e}\right) \tag{10}$$

where R is the universal gas constant (8.314 J/mol/K), T is the temperature (K) and C_e is the equilibrium concentration of TC in liquid (mol/L).

The linear form of Eq. (9) is given as:

$$\ln q_e=\ln q_{\text{DR}}-K_{\text{DR}}\varepsilon^2 \tag{11}$$

The mean adsorption energy (E) can be computed using Eq. (12):

$$E = \frac{1}{\sqrt{2K_{DR}}} \tag{12}$$

The mean adsorption energy gives an idea about type of adsorption: physical or chemical. If the mean adsorption energy value is lower than 8 kJ/mol, the adsorption is assumed to be physical nature while it is assumed to be chemical adsorption for values between 8 and 16 kJ/mol [17].

2.7. Adsorption kinetics

In this study, various kinetic models including pseudo-first-order, pseudo-second-order, intraparticle diffusion and Elovich kinetic models were used to find out the possible mechanism for TC adsorption.

The pseudo-first-order kinetic model known as the Lagergren model [39] is expressed as follows:

$$\frac{dq_t}{dt} = k_1\left(q_e - q_t\right) \tag{13}$$

where k_1 is the rate constant of pseudo-first-order model (1/min). The linearized form of Eq. (13) becomes as follows:

$$\log\left(q_e - q_t\right) = \log q_e - \frac{k_1}{2.303}t \tag{14}$$

The pseudo-second-order model proposed by Ho and McKay [40] is expressed as follows:

$$\frac{dq_t}{dt} = k_2\left(q_e - q_t\right)^2 \tag{15}$$

where k_2 is the rate constant of pseudo-second-order model (g/mg/min). The linearized form of Eq. (15) becomes as follows:

$$\frac{t}{q_t} = \frac{1}{k_2 q_e^2} + \frac{1}{q_e}t \tag{16}$$

Intraparticle diffusion equation, developed by Weber and Morris [41] is expressed with the following relationship:

$$q_t = k_{id}t^{0.5} + C_i \tag{17}$$

where k_{id} and C_i represent the intraparticle diffusion rate constant (mg/g/min$^{1/2}$) and a constant giving information about the boundary layer thickness (mg/g), respectively.

The Elovich model is valid for systems with heterogeneous surface and it is suitable and applicable for chemisorption kinetics [42]. The linearized form of the Elovich model is expressed with the following relationship:

$$q_t = \frac{1}{\beta}\ln\alpha\beta + \frac{1}{\beta}\ln t \tag{18}$$

where α is the initial adsorption rate (mg/g/min) and β is the constant related to the extent of surface coverage and the activation energy for chemisorption (g/mg).

In order to further verify the best-fit kinetic model of adsorption, the normalized standard deviation (SD) for the kinetic models was assessed by using Eq. (19).

$$\mathrm{SD}(\%) = 100\sqrt{\frac{\sum\left(\frac{q_{e,\exp} - q_{e,\mathrm{cal}}}{q_{e,\exp}}\right)^2}{N-1}} \tag{19}$$

where $q_{e,\exp}$ and $q_{e,\mathrm{cal}}$ (mg/g) are the experimental and calculated equilibrium adsorption capacities, respectively and N is the number of data points.

2.8. Adsorption thermodynamics

As known, thermodynamic parameters give information about the suitability and spontaneous nature of the process. To determine the nature of adsorption process for TC adsorption onto chitin, the thermodynamic parameters including the changes in Gibbs free energy ($\Delta G°$), standard enthalpy ($\Delta H°$) and entropy ($\Delta S°$) were calculated using Eqs. (20) and (21):

$$\Delta G° = -RT\ln K \tag{20}$$

$$\ln K_L = \frac{\Delta S°}{R} - \frac{\Delta H°}{RT} \tag{21}$$

where $\Delta G°$ is kJ/mol, $\Delta S°$ is kJ/mol/K, $\Delta H°$ is kJ/mol and K_L is the equilibrium constant (the Langmuir constant). $\Delta H°$ and $\Delta S°$ could be determined from the slope and intercept of $\ln K_L$ vs. $1/T$ plot, respectively [43].

2.9. Desorption and recycle studies of chitin

The desorption experiments were performed using several desorbing agents, including the water, methanol, ethanol, 50% water/50% methanol, 50% water/50% ethanol, 0.01 M HCl and 0.01 M NaOH as eluents. Initially, after adsorption of TC by chitin was achieved using TC concentration of 20 mg/L at initial solution pH of 7 and chitin dosage of 5 g/L, the adsorbed amount was calculated. Then, the TC-loaded chitin was separated from liquid phase by centrifugation. In order to remove the unadsorbed fraction of the TC molecules onto chitin, the chitin separated from the liquid was washed with distilled water and dried for 15 h at 50°C. Then, 0.25 g of TC-loaded chitin was added to 50 mL of the desorbing agents and the mixture was shaken in an orbital shaker for 2 h. After this process, the samples were centrifuged at 1,500 rpm for 2 min and filtered through 0.22-μm membrane syringe filter to determine TC concentration by HPLC. The percentage of TC desorbed from the chitin was calculated using formula as presented. In addition, multiple recycle study containing adsorption and desorption was also conducted using water, 0.01 M NaOH and 0.01 M HCl as desorbing agents. The spent adsorbents after each cycle were treated with these desorbing agents, followed by thorough washing with distilled and then used for the next cycle. This adsorption–desorption cycle was repeated

four times. The desorption capacity of TC ($q_{desorption}$, mg/g) was calculated according to Eq. (22):

$$q_{desorption} = \frac{V \cdot C_{des}}{m} \quad (22)$$

where $q_{desorption}$ is the amount of TC desorbed from 1 g of saturated chitin (mg/g), C_{des} is the concentration of TC in the desorption solution (mg/L), V is the volume of eluent solution (L) and m is the mass of the TC-saturated chitin (g).

The desorption efficiency (%) of TC was calculated using Eq. (23):

$$\text{Desorption efficiency}\,(\%) = \left(\frac{q_{desorption}}{q_{adsorption}}\right) \times 100 \quad (23)$$

3. Results and discussion

3.1. Characteristics of chitin

The SEM images belonging to chitin before and after TC adsorption are shown in Fig. 2. As seen from SEM images, the chitin displayed different surface characteristics. Before TC adsorption, the chitin surface shows porous and heterogeneous structure and the pores had random distribution throughout the surface. After adsorption of TC, the surface of the chitin appeared to be rough in nature. This may be due to the formation of TC-chitin complex. Energy-dispersive x-ray of chitin before and after adsorption with TC was analyzed. As seen in Fig. 2a and b, the elemental analysis of the chitin is shown that C and O are main constituents and after adsorption, the contents of C and O increased which is evident the tetracycline adsorption. The copper was potentially impurities from the sieves while the gold resulted from the analysis used in energy-dispersive X-ray spectroscopy.

The chemical structure and functional group information for adsorbents can be analyzed from the FTIR spectra. The FTIR spectra of chitin before and after TC adsorption are given in Fig. 3. There was a wide absorption peak observed at 3,423 cm^{-1} for chitin, mainly assigned to the –OH stretching vibration [44]. In the spectra of chitin, the peak observed at around 3,140 cm^{-1} corresponds to the N–H stretching vibration. Moreover, the peaks at 2,927 and

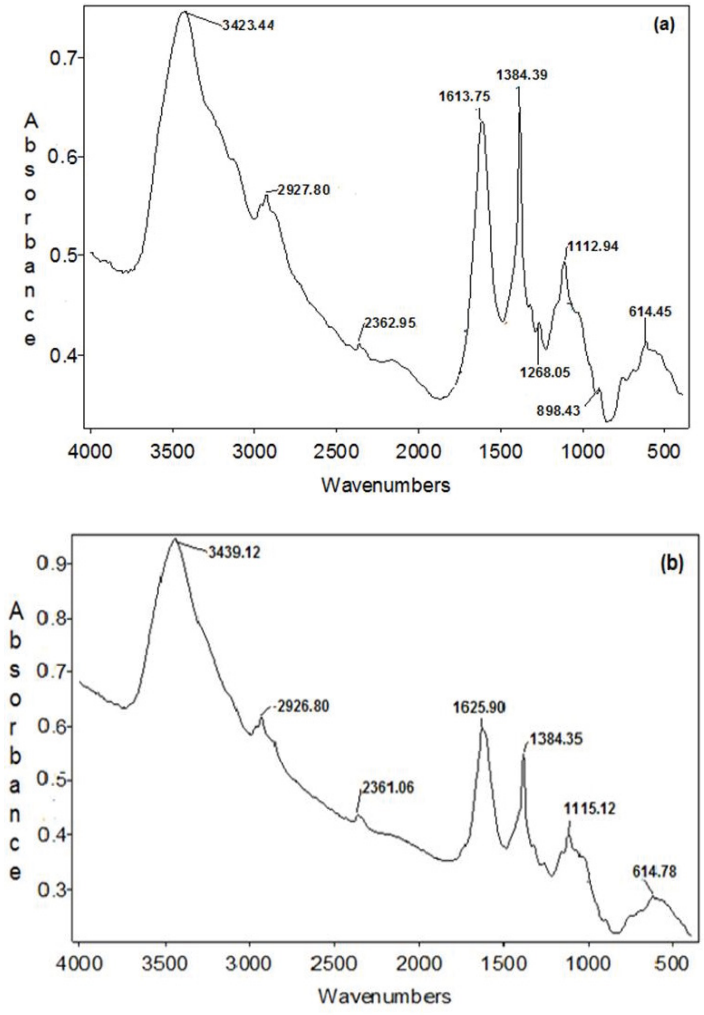

Fig. 2. FTIR spectra of chitin (a) before and (b) after TC adsorption.

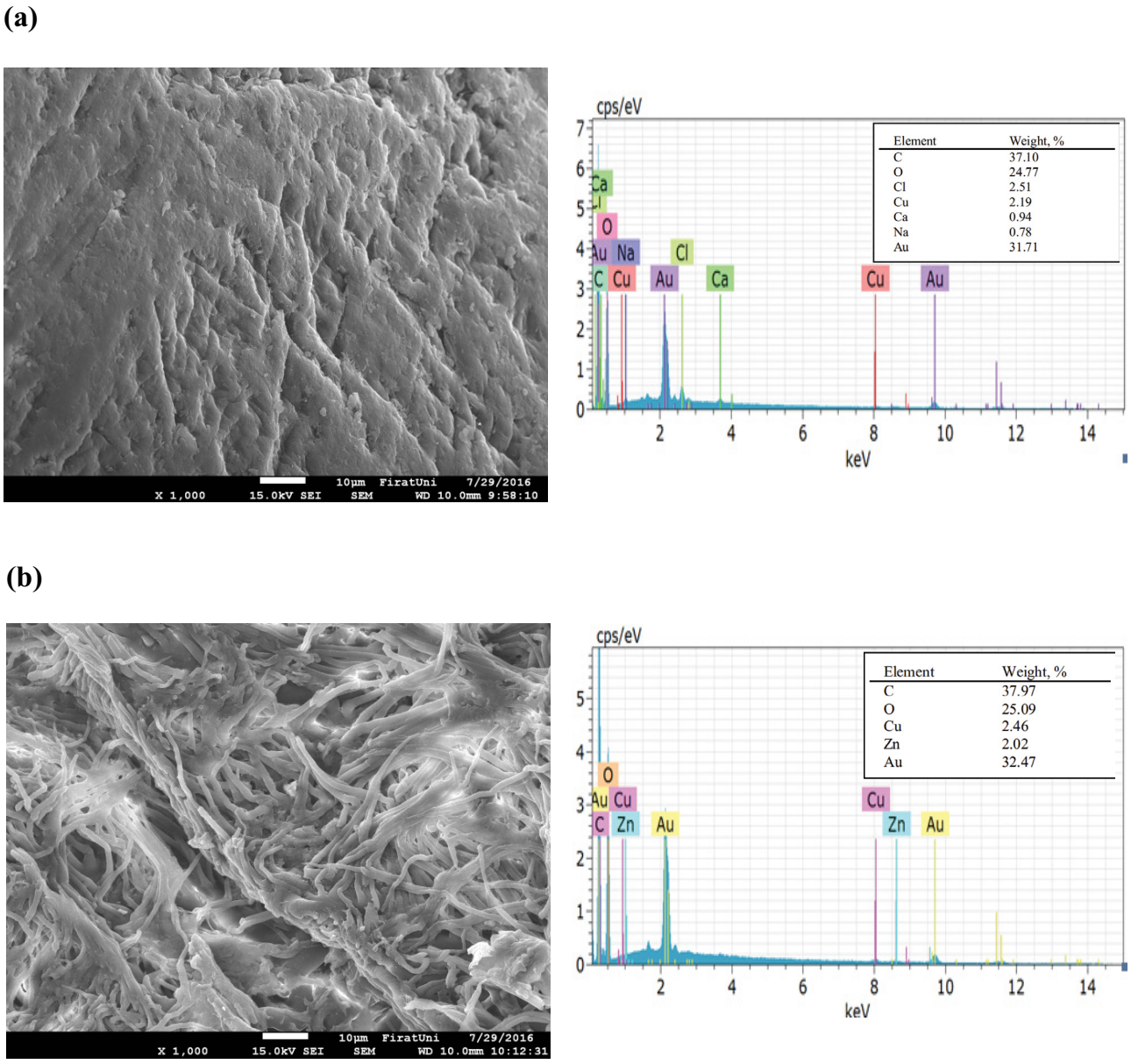

Fig. 3. SEM images and energy-dispersive X-ray spectra of chitin (a) before and (b) after TC adsorption.

1,384 cm^{-1} were related to the C–H stretching and the C–H bending vibrations, respectively. The band at 1,384 cm^{-1} can be assigned to $–CH_3$ deformation modes of the N-acetyl group. The peak that indicates the C–N stretching vibration appeared at 1,268 cm^{-1}. The band at 1,113 cm^{-1} can be assigned to C–O and C–C stretching modes of COH and COC in the pyranose ring. The band at 897 cm^{-1} can be ascribed to the C–O stretching of glycosidic bond [28]. Similar peaks for chitin were also recorded in other studies [28,45,46]. The changes in the FTIR spectra of the chitin occurred after TC adsorption. A clear shift in peak from 3,423 to 3,439 cm^{-1}, corresponding to the stretching vibrations of the O–H was observed. Moreover, the differences in the intensity of peaks were also observed. These results can be related to interaction between chitin and TC.

The BET surface area, the pore volume and the pore diameter of chitin was determined as 6.667 m^2/g, 0.02506 cm^3/g and 17.962 nm, respectively. The length, width, and thickness of TC molecules are 1.41, 0.46 and 0.81 nm, respectively [47]. It was clear that chitin had a range of pore sizes for the adsorption of TC molecules.

3.2. Influence of initial pH

The pH of adsorption medium is a significant parameter for adsorption process which affects not only the surface charge of the adsorbents but also the ionization forms of adsorptive molecule in the solution [48]. Hence, it was a significant data affecting the adsorption behavior, the effect of initial pH on the adsorption of TC by

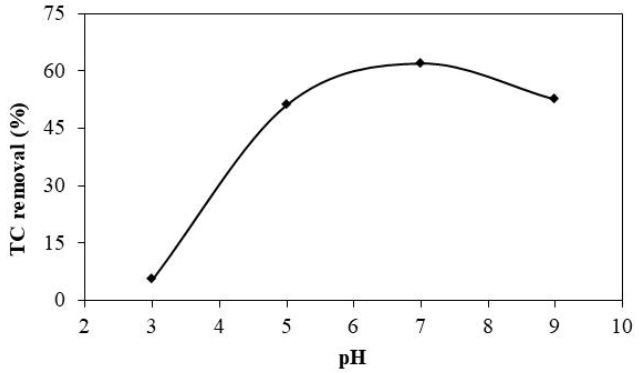

Fig. 4. Effect of initial pH of the solution on adsorption of TC by chitin.

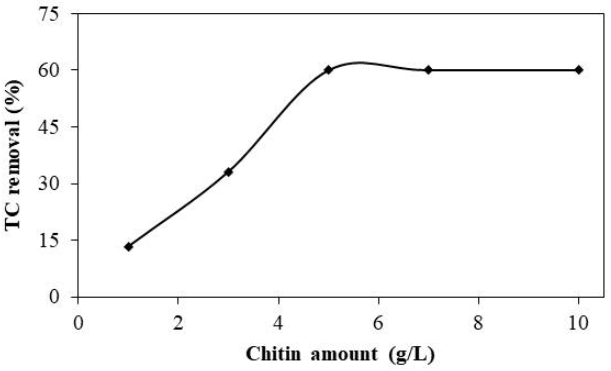

Fig. 5. Effect of chitin amount on the adsorption of TC by chitin.

chitin was examined between 3 and 9. Fig. 4 shows the variation of TC removal according to the initial pH. From Fig. 4, the adsorption efficiency of chitin for TC first increased at pH from 3 to 7 and decreased at pH of 9. This could be interpreted by the electrostatic interaction between the TC and chitin in an aqueous solution with varying pH. The pKa values are 3.3, 7.7, and 9.7 for TC molecule [15,49]. Therefore, TC in aqueous solutions exists as cationic species (pH < 3.3), zwitter-ionic species (3.3 < pH < 7.7) and anionic species (7.7 > pH) [17]. On the other hand, the pH_{pzc} of chitin is approximately 5.4–7.2 [50–52]. Hence, chitin becomes positively charged at pH < pH_{pzc} and negatively charged at pH > pH_{pzc}. When the solution pH is below the pKa_1 (3.3) value of TC, TC in the solution exists as cationic species, while the surface of the adsorbent is positively charged, resulting in a strong electrostatic repulsion. Therefore, the low adsorption efficiency was inevitable at pH 3. However, at high pH values, as TC molecule is negatively charged, interaction between the adsorbent surface and TC molecules is weak and thus, diminishes the adsorption efficiency. On the other hand, TC is the form of the zwitter-ion at pH 7. Adsorption mechanism for TC adsorption in this condition can attribute surface complexation (e.g., H-bonding). In the H-bonding formation, the functional groups such as $–CH_3$, –OH, $–NH_2$ and N–H in the TC molecule in the binding of TC onto chitin may act as H acceptor interacting with the O-containing groups such as C=O in the surface by H-bonding [17]. Based on the above-discussion, the optimal solution pH value was 7.

3.3. Influence of chitin amount

The effect of chitin amount on TC adsorption is shown in Fig. 5. Obviously, TC adsorption performance increased with the increasing chitin amount up to 5 g/L and then reached a constant value. The adsorption efficiencies for TC by chitin were 13% and 60%, respectively, at a chitin dosage of 1 and 5 g/L. This significant adsorption efficiency improvement was mainly attributed to the interface contact area between the chitin and TC molecules being relatively due to more available active sites area by the increasing chitin dosage [53].

3.4. Influence of temperature

To evaluate the influence of temperature on the adsorption capacity of chitin, a series of experiments were conducted with initial TC concentrations of 10–80 mg/L in the range of 25°C–55°C at 5 g/L chitin dosage and pH 7. As presented in Table 1, an increase in the temperature from 25°C to 55°C led to an increase in the equilibrium sorption capacity from 1.20 to 1.36 mg/g and from 5.88 to 7.08 mg/g for chitin at the initial TC concentrations of 10 and 80 mg/L, respectively. Similar results were also obtained for TC adsorption efficiencies. For example, the adsorption efficiencies were obtained to be 59.9%, 63.6% and 68.2% at the initial TC concentration of 10 mg/L for 25°C, 40°C and 55°C, respectively (Table 1). The increase of the adsorption capacity and adsorption efficiency with the increase of the temperature could be related with the enlargement of pore size or increase in number of active sites on the adsorbent surface. This also demonstrated that the adsorption of TC onto chitin is an endothermic process. On the other hand, it could be also due to the decrease in the thickness of the boundary layer surrounding the sorbent with temperature, thus the mass transfer resistance of adsorbate in the boundary layer decreases. This may also be a result of high mobility of the TC molecule with an increase in their kinetic energy, and the enhanced rate of intraparticle diffusion of sorbate with the rise of temperature [54].

3.5. Influence of initial TC concentration

The influence of the initial concentration of TC on the adsorption capacity by chitin is shown in Table 1. With initial TC concentrations ranging from 10–80 mg/L at 25°C, the adsorption capacity by chitin increased from 1.2 to 5.88 mg/g. As the initial adsorbate concentration ensures a high driving force to overcome all mass transfer resistance between the aqueous and solid phases, a raise in the initial adsorbate concentration enhances the adsorption capacity [54]. Additionally, increasing initial adsorbate concentration increases the number of collisions between adsorbate and adsorbent [55]. As seen in Table 1, the equilibrium adsorption capacity of chitin enhanced with increasing initial TC concentration from 10 to 80 mg/L at all temperatures owing to the increase in the number of ions contending for existing binding sites on adsorbent. On the other hand, an

Table 1
The equilibrium uptake capacities and adsorption yields obtained at different initial concentrations and temperature

C_0 (mg/L)	25°C		40°C		55°C	
	q_e (mg/g)	Adsorption (%)	q_e (mg/g)	Adsorption (%)	q_e (mg/g)	Adsorption (%)
10	1.20	59.9	1.27	63.6	1.36	68.2
20	2.05	51.4	2.16	54.0	2.39	59.9
40	3.74	46.7	3.76	47.1	4.60	57.5
60	4.58	38.2	4.84	40.3	5.87	49.0
80	5.88	36.8	6.12	38.2	7.08	44.2

increase in TC concentration generally led to decreasing in TC adsorption efficiency. At temperature of 55°C, TC removal efficiency was 68.2% at the initial concentration of 10 mg/L while it was determined to be 44.2% at the initial concentration of 80 mg/L. This could be related with a great majority of adsorbate in the adsorption medium which can interact with the binding sites at lower concentrations. Moreover, the saturation of sorption sites occurred at higher TC concentrations.

3.6. Modeling of adsorption equilibrium

Various adsorption isotherm models can be used to investigate how the interaction between adsorbate and adsorbent can employ and to provide information about the capacity of adsorbent, and also to understand the mechanism of adsorption [35]. In this study, Langmuir, Freundlich, and Dubinin–Radushkevich for modeling of the adsorption data were examined. Initial TC concentrations were altered from 10 to 80 mg/L while the chitin amount was kept constant (5 g/L) at 25°C, 40°C and 55°C in order to determine the equilibrium isotherms. The isotherm parameters and regression coefficients (R^2) determined from the linear plot of Langmuir (C_e/q_e vs. C_e) (Fig. 6a), Freundlich ($\ln q_e$ vs. $\ln C_e$) (Fig. 6b), and Dubinin–Radushkevich isotherm ($\ln q_e$ vs ε^2) (Fig. 6c) of TC adsorption onto chitin were listed in Table 2. The maximum adsorption capacity of TC onto chitin determined from the Langmuir model was obtained as 8.84, 8.93 and 10.91 mg/g at 25°C, 40°C and 55°C, respectively. For adsorption of TC by chitin, the highest K_L value at the studied temperatures was obtained to be 0.0402 L/mg at 55°C. As seen in Table 2, q_{max} and K_L values increased with raising temperature. The values of R_L by using Eq. (6) were in the ranges of 0.746–0.237 (Fig. 7). These results demonstrated that the chitin is favorable for adsorption of TC in the concentration and temperature studied. Additionally, the K_F values determined from Freundlich isotherm model was gradually increased from 0.507 to 0.660 with the temperature rising. As seen in Table 2, n values were greater than 1, it can be inferred the adsorption process was favorable.

The adsorption energy was calculated as 10.0, 11.2 and 11.2 kJ/mol at temperatures of 25°C, 40°C and 55°C, respectively by applying Dubinin–Radushkevich isotherm model. The magnitudes of E were between 8 and 16 kJ/mol, which indicate that the adsorption process of TC onto chitin could be chemical adsorption. Although the regression coefficients ($R^2 \geq 0.95$) of three equations (Langmuir, Freundlich

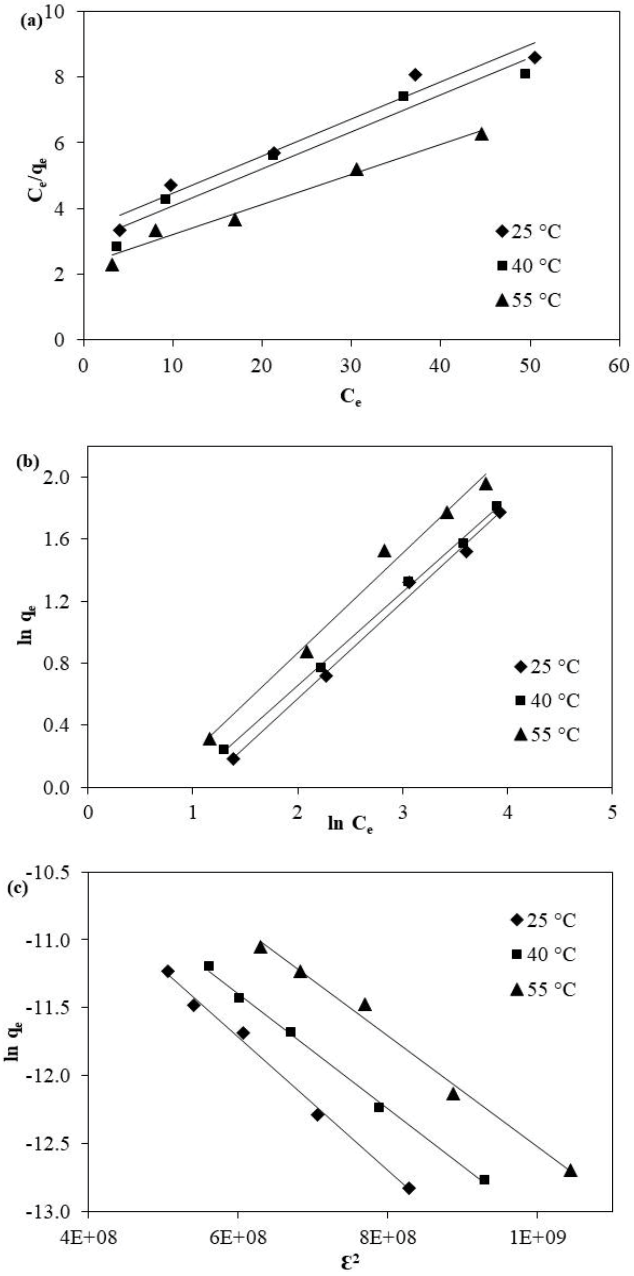

Fig. 6. Linear plot of isotherm models for TC adsorption by chitin (a) Langmuir, (b) Freundlich and (c) Dubinin–Radushkevich isotherms.

and Dubinin–Radushkevich) are quite well obtained, it is obvious from Table 2 that the Freundlich and Dubinin–Radushkevich isotherm models exhibited best fit to the adsorption data than Langmuir model. From these results, it is seen that TC was adsorbed onto chitin as multilayer adsorption on heterogeneous surface. SEM results also showed that the chitin has heterogeneous surface.

3.7. Modeling of adsorption kinetics

To investigate the adsorption behavior of TC in the adsorption process, four kinetic models including the pseudo-first-order, the pseudo-second-order, the intraparticle diffusion and the Elovich models have been used to fit the data. The pseudo-first-order model was based on the hypothesis that the adsorption rate was positively correlated with adsorption sites, while the pseudo-second-order model assumes that the adsorption rate was determined by the square of adsorption sites on the surface of adsorbents [56].

The plots of linearized form of the pseudo-first-order and the pseudo-second-order models are shown in Fig. 8a and b, respectively. The k_1 and q_e values of the pseudo-first-order model were found from the plot of $\log(q_e - q_t)$ vs. t while the k_2 and q_e values of the pseudo-second-order model were determined from the plot of t/q vs. t. The k_1, k_2, q_e and regression coefficients (R^2) calculated from these models are given in Table 3. The regression coefficient for the pseudo-first-order kinetic model obtained at 55°C was very low.

The intraparticle diffusion model assumes that the adsorption occurs via the diffusion of adsorbate molecules into the pores of adsorbent [10] and intraparticle diffusion is the sole rate-controlling process [57]. The plots of q_t vs. $t^{0.5}$ (undisclosed data) deduced that the plots had multi-linearity. The first linear partition at the initial period is attributed to the diffusion of TC adsorbed on the external surface of the chitin from the solution or the border layer diffusion of the solute molecules. The second linear partition being an indicator of the intraparticle diffusion shows the gradual layer adsorption stage. The third plateau partition describes the final equilibrium stage representing the slowing down internal diffusion owing to the low TC concentration left in the solution. Linear plots of the second partition did not pass through the origin. This indicates that the border layer control had some steps, and

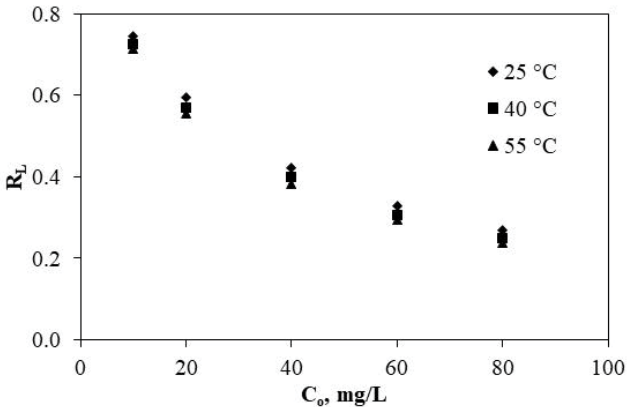

Fig. 7. Variation of separation factor (R_L) with initial TC concentration and temperature.

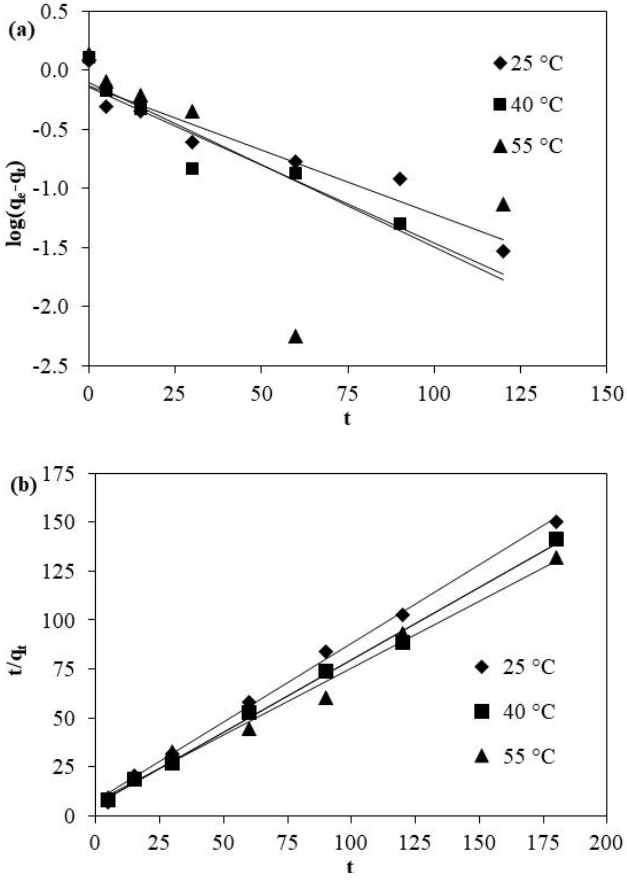

Fig. 8. Linear plot of kinetic models for TC by chitin (a) pseudo-first-order and (b) pseudo-second-order.

Table 2
Isotherm parameters and regression coefficients of Langmuir, Freundlich, and Dubinin–Radushkevich isotherm models for adsorption of TC onto chitin

T (°C)	Langmuir model			Freundlich model			Dubinin–Radushkevich model			
	q_{max} (mg/g)	K_L (L/mg)	R^2	K_F	n	R^2	q_{DR} (mol/g)	K_{DR} (mol²/J²)	E (kJ/mol)	R^2
25	8.84	0.0341	0.9587	0.507	1.601	0.9932	1.6×10^{-4}	5×10^{-9}	10.0	0.9941
40	8.93	0.0377	0.9583	0.583	1.667	0.9983	1.4×10^{-4}	4×10^{-9}	11.2	0.9969
55	10.91	0.0402	0.9786	0.660	1.561	0.9880	2.2×10^{-4}	4×10^{-9}	11.2	0.9910

Table 3
Kinetic parameters and regression coefficients of pseudo-first-order, pseudo-second-order, intraparticle diffusion and Elovich models for TC adsorption onto chitin

T (°C)	$q_{e,exp}$ (mg/g)	First-order kinetic model			Second-order kinetic model		
		k_1 (1/min)	$q_{e,cal}$ (mg/g)	R^2	k_2 (g/mg/min)	$q_{e,cal}$ (mg/g)	R^2
25	1.20	0.0249	0.73	0.919	0.0897	1.24	0.997
40	1.27	0.0320	0.79	0.892	0.0966	1.35	0.995
55	1.36	0.0302	0.97	0.445	0.0668	1.46	0.988
T (°C)		Intraparticle diffusion model			Elovich model		
		k_{id} (mg/g/min$^{0.5}$)	C_i (mg/g)	R^2	α (mg/g/min)	b (mg/g)	R^2
25		0.0534	0.593	0.953	2.600	6.734	0.954
40		0.0791	0.519	0.897	0.910	4.876	0.924
55		0.1364	0.228	0.984	0.395	3.761	0.869

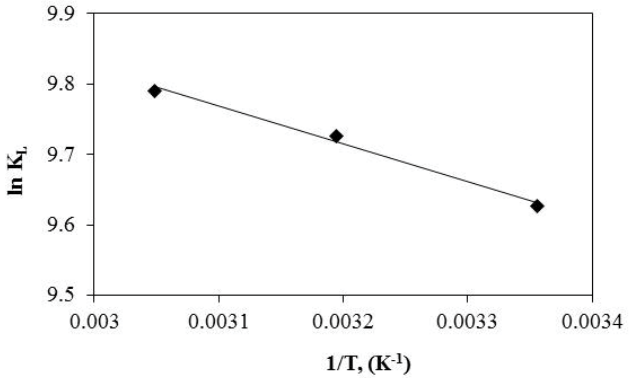

Fig. 9. Plot of lnK_L vs. 1/T.

it also shows that intraparticle diffusion was present, but was not the step solely controlling the rate [17,58]. The similar results showed that the intraparticle diffusion was involved, but is not the only rate-limiting step in the adsorption process of ibuprofen by modified chitin [33].

The intraparticle diffusion rate constants obtained from the slope of linear partition of the plots increased with the increase in temperature as shown in Table 3. The Elovich model suggests the heterogeneous chemisorption of the adsorbate onto the solid adsorbent [57]. α and β values and regression coefficients calculated from the plots of q_t vs. ln(t) are also presented in Table 3. The values of regression coefficient of the pseudo-second-order model were the highest among the other models. The calculated q_e values obtained from pseudo-second-order model agreed well with the experimental q_e values. It should be emphasized that the pseudo-second-order kinetic model is a consequence of the cooperative effects of the adsorption steps: (i) mass transfer of adsorbate from solution to the boundary film; (ii) mass transfer of adsorbate from boundary film to surface or diffusion across the film surrounding the surface of the sorbent; (iii) diffusion in the pores of the sorbent: sorption or ion exchange of ions onto sites; and finally (iv) adsorption of adsorbate onto the sorbent surface [59]. Also, SD values were determined by Eq. (19) and it was found that SD value of pseudo-second-order kinetic (SD = 7.2) was lower than that of the pseudo-first-order model (SD = 43.5). The higher the value of R^2 and the lower the value of SD, the better the model fits the experimental data [33]. These results showed that the adsorption process can be described by the pseudo-second-order kinetic model.

Table 4
ΔG° values for adsorption of TC onto chitin at different temperatures

T (°C)	K_L (L/mg)	ΔG° (kJ/mol)
25	0.0341	–23.85
40	0.0377	–25.31
55	0.0402	–26.70

3.8. Thermodynamic evaluation

The Gibbs free energy changes were calculated by using the equilibrium constants of Langmuir model. As seen from Table 4, all Gibbs free energy values were negative that show the adsorption was a spontaneous and favorable process. And the values of ΔG° were gradually decreased with the temperature increasing, which indicated that the higher temperature was beneficial to adsorption process. The standard enthalpy change of adsorption obtained from the lnK_L vs. 1/T plot (Fig. 9) was found as 4.47 kJ/mol. This positive ΔH° value indicates that TC adsorption process onto chitin has the endothermic nature. Moreover, the entropy change of adsorption was determined to be 0.095 kJ/mol/K which demonstrates the affinity of chitin for TC and the increasing randomness at the solid-solution interface during adsorption process. Similar findings were reported by Liu et al. [25] using nitrogen rich hollow carbon spheres using as a sorbent of TC.

3.9. Insight into TC removal by chitin

3.9.1. Adsorption mechanism

The research of adsorption mechanism was beneficial to understand the adsorption process of TC onto chitin. Fig. 10

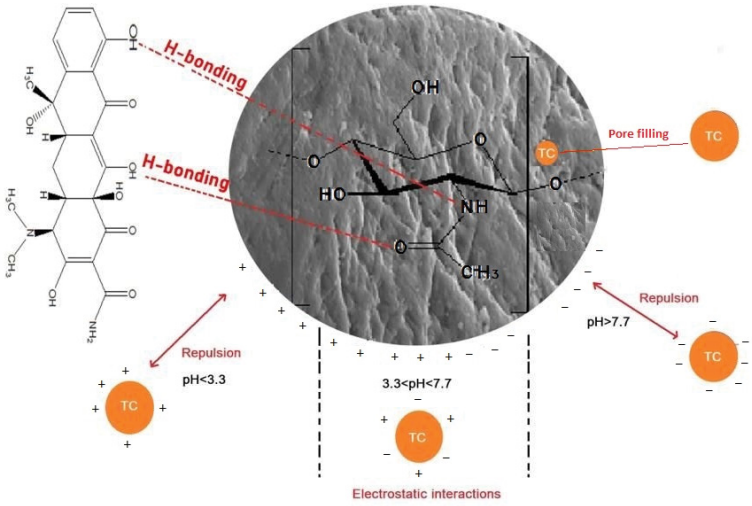

Fig. 10. The possible adsorption mechanism for tetracycline onto chitin.

illustrated the possible adsorption mechanism for tetracycline onto chitin. Firstly, TC is a tribasic acid, and its three acid dissociation constants are 3.3, 7.7, and 9.7. Therefore, TC will appear in different charged ion forms under different pH environments. While, both chitin and TC are positively charged for pH < 3.3, for pH > 7.7, both are negatively charged. At this time, the adsorption effect between the two is weakened due to electrostatic repulsion [60]. As depicted in Fig. 4, it can be seen that the optimal pH value was pH 7 for TC adsorption and TC is the form of the zwitterion under this condition. Hence, a weak electrostatic interactions can be occurred between TC molecule and adsorbent and at this stage, the adsorption both the two is more likely to involve an intermolecular interaction [49]. Furthermore, pH_{pzc} of chitin was not directly related to the adsorption results, confirming that the electrostatic interaction force was not dominant in TC adsorption by chitin at pH: 7. Secondly, the oxygen-containing functional groups (hydroxyl, carbonyl, etc.) in chitin can participate in the TC adsorption process through hydrogen bonding during the adsorption process. By considering the FTIR results, there was a shift in some peaks and differences in the peak intensity. For example, before adsorption, the peaks observed at 3,423 and 1,613 cm^{-1} were shifted to 3,439 and 1,626 cm^{-1} after adsorption. These observations confirm the interaction between chitin and TC. Lastly according the pore sizes of TC and chitin, pore filling can contribute the adsorption process. To sum up, the adsorption process of TC was determined by multiple reaction mechanism including pore filling, hydrogen bonding and weak electrostatic attraction.

3.9.2. Desorption and recycle results of chitin

The reusability of an adsorbent plays an important role in practical application and greatly increases the attractiveness of its use. For this purpose, desorption and recycle studies were also performed to evaluate reusability of chitin. The percentages of TC desorbed from chitin are shown in Fig. 11. The desorption percentages increased

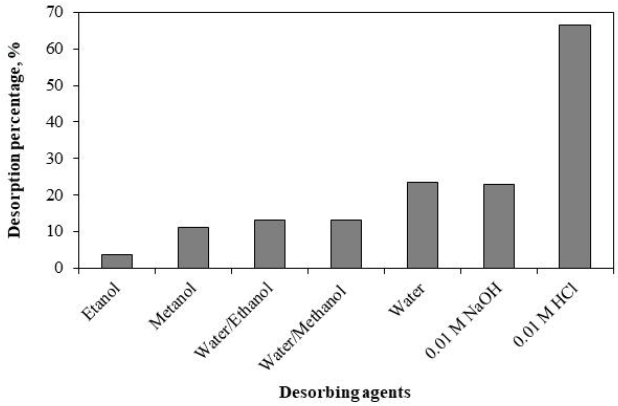

Fig. 11. Desorption efficiency of TC from chitin depending on the desorbing agents.

in the following order: ethanol < methanol < water/ethanol < water/methanol < water < 0.01 M NaOH < 0.01 M HCl. The highest desorption percentage was obtained by 0.01 M HCl (66.6%). The reusability of chitin was tested during consecutive adsorption–desorption cycle using desorbing agents that include water, 0.01 M NaOH and 0.01 M HCl as eluent. The adsorption efficiencies of chitin after each adsorption–desorption cycle are shown in Fig. 12. The original adsorption efficiency of chitin for TC was 51.4%. When water, 0.01 M NaOH and 0.01 M HCl as desorbing agents were used, the TC adsorption efficiency decreased to 21%, 27% and 1%, respectively after the four cycles. The possible reasons for this may be the morphological alteration and the degradation of the active sites, with consecutive cycles. Some amount of TC does not desorb during the desorption cycles, with each cycle such molecules tend to block the activate sites, making them unavailable for the consecutive cycles [61].

Among the studied desorbing agents, 0.01 M HCl was efficient for desorbing TC from the chitin. However, TC adsorption by chitin regenerated using 0.01 M HCl was

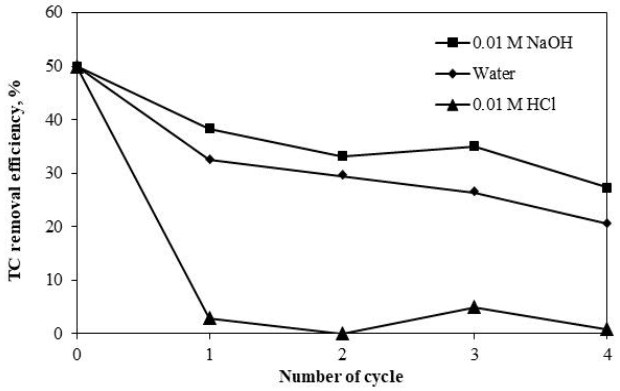

Fig. 12. Reusability of chitin for TC adsorption.

not achieved. This may be due to the deterioration of some functional structures of chitin by treatment of HCl and losing the adsorption capacity. Especially, this phenomenon may be a result of the hydrolysis reaction. There are some studies stating that chitin hydrolyzes under concentrated acidic conditions [62,63]. It has been concluded that acidic washing solutions are not suitable for the regeneration of the chitin.

4. Conclusions

Combining the characterization results and the results from the adsorption experiments, we concluded that weak electrostatic attraction, hydrogen bonds and pore filling involved in the adsorption mechanisms. The adsorption capacity of chitin was affected by initial pH, temperature and initial TC concentrations. Although chitin has low sorption capacity of TC, it does not preclude its use as an effective sorbent. Because there was no need to adjust pH value after adsorption process since the optimum pH was found to be 7 for TC adsorption by chitin. The adsorption of TC onto chitin fitted well to Freundlich isotherm while the adsorption kinetic of TC removal by chitin followed the pseudo-second-order model. The intraparticle diffusion model suggests that intraparticle diffusion is not the only rate controlling step. The negative value of $\Delta G°$ indicates that adsorption process has spontaneous nature. The positive value of $\Delta H°$ shows that adsorption process is endothermic. Recyclability studies verified the loss in adsorption efficiency of chitin towards TC after consecutive cycles. In the further study, some methods to modify the chitin surface structure should be explored to improve the adsorption capacity of chitin.

Acknowledgments

We thank Assistant Professor Dr. Şeyda Taşar from Firat University, Faculty of Engineering, Department of Chemistry Engineering, Elazig/Turkey for FTIR analyses and Res. Assoc. Dr. Burçin Yıldız from Van Yuzuncu Yil University, Faculty of Engineering and Architecture, Department of Environmental Engineering, Van/Turkey for her assistance in the HPLC analyses.

References

[1] Z. Li, L. Schulz, C. Ackley, N. Fenske, Adsorption of tetracycline on kaolinite with pH-dependent surface charges, J. Colloid Interface Sci., 351 (2010) 254–260.
[2] Z. Zhang, K. Sun, B. Gao, G. Zhang, X. Liu, Y. Zhao, Adsorption of tetracycline on soil and sediment: effects of pH and the presence of Cu(II), J. Hazard. Mater., 190 (2011) 856–862.
[3] Y. Gao, Y. Li, L. Zhang, H. Huang, J. Hu, S.M. Shah, X. Su, Adsorption and removal of tetracycline antibiotics from aqueous solution by graphene oxide, J. Colloid Interface Sci., 368 (2012) 540–546.
[4] V.H.T. Thi, B.-K. Lee, Great improvement on tetracycline removal using ZnO rod-activated carbon fiber composite prepared with a facile microwave method, J. Hazard. Mater., 324 (2017) 329–339.
[5] J. Cao, Z.H. Yang, W.P. Xiong, Y.Y. Zhou, Y.R. Peng, X. Li, C.Y. Zhou, R. Xu, Y.R. Zhang, One-step synthesis of Co-doped UiO-66 nanoparticle with enhanced removal efficiency of tetracycline: simultaneous adsorption and photocatalysis, Chem. Eng. Commun., 353 (2018) 126–137.
[6] H. Peng, J. Cao, W. Xiong, Z. Yang, M. Jia, S. Sun, Z. Xu, Y. Zhang, H. Cai, Two-dimension N-doped nanoporous carbon from KCl thermal exfoliation of Zn-ZIF-L: efficient adsorption for tetracycline and optimizing of response surface model, J. Hazard. Mater., 402 (2021) 123498, doi: 10.1016/j.jhazmat.2020.123498.
[7] S.J. Jiao, S.R. Zheng, D.Q. Yin, L.H. Wang, L.Y. Chen, Aqueous photolysis of tetracycline and toxicity of photolytic products to luminescent bacteria, Chemosphere, 73 (2008) 377–382.
[8] L. Gao, L.J. Shi, T. Yuan, Growth inhibitive effect of typical antibiotics and their mixtures on *Selenastrum capricornutum*, J. Environ. Health, 30 (2013) 475–478.
[9] H. Li, J. Hu, Y. Meng, J. Su, X. Wang, An investigation into the rapid removal of tetracycline using multi layered graphene-phase biochar derived from waste chicken feather, Sci. Total Environ., 603–604 (2017) 39–48.
[10] A.C. Martins, O. Pezoti, A.L. Cazetta, K.C. Bedin, D.A.S. Yamazaki, G.F.G. Bandoch, T. Asefa, J.V. Visentainer, V.C. Almeida, Removal of tetracycline by NaOH-activated carbon produced from macadamia nut shells: kinetic and equilibrium studies, Chem. Eng. J., 260 (2015) 291–299.
[11] M.H. Khan, H. Bae, J.-Y. Jung, Tetracycline degradation by ozonation in the aqueous phase: proposed degradation intermediates and pathway, J. Hazard. Mater., 181 (2010) 659–665.
[12] E. Yamal-Turbay, E. Jaén, M. Graells, M. Pérez-Moya, Enhanced photo-Fenton process for tetracycline degradation using efficient hydrogen peroxide dosage, J. Photochem. Photobiol., A, 267 (2013) 11–16.
[13] S. Liu, X. Zhao, H. Sun, R. Li, Y. Fang, Y. Huang, The degradation of tetracycline in a photo-electro-Fenton system, Chem. Eng. J., 231 (2013) 441–448.
[14] Y.A. Ouaissa, M. Chabani, A. Amrane, A. Bensmaili, Removal of tetracycline by electrocoagulation: kinetic and isotherm modeling through adsorption, J. Environ. Chem. Eng., 2 (2014) 177–184.
[15] Q. Zhou, Z. Li, C. Shuang, A. Li, M. Zhang, M. Wang, Efficient removal of tetracycline by reusable magnetic microspheres with a high surface area, Chem. Eng. J., 210 (2012) 350–356.
[16] P. Sathishkumar, M. Arulkumar, V. Ashokkumar, A.R.M. Yusoff, K. Murugesan, T. Palvannan, Z. Salam, F. Nasir Ani, T. Hadibarata, Modified phyto-waste *Terminalia catappa* fruit shells: a reusable adsorbent for the removal of micropollutant diclofenac, RSC Adv., 5 (2015) 30950–30962.
[17] H. Sayğılı, F. Güzel, Effective removal of tetracycline from aqueous solution using activated carbon prepared from tomato (*Lycopersicon esculentum* Mill.) industrial processing waste, Ecotoxicol. Environ. Saf., 131 (2016) 22–29.
[18] B. Li, Y. Zhang, J. Xu, Y. Mei, S. Fan, H. Xu, Effect of carbonization methods on the properties of tea waste biochars and their application in tetracycline removal from aqueous solutions, Chemosphere, 267 (2021) 129283, doi: 10.1016/j.chemosphere.2020.129283.

[19] X. Sheng, J. Wang, Q. Cui, W. Zhang, X. Zhu, A feasible biochar derived from biogas residue and its application in the efficient adsorption of tetracycline from an aqueous solution, Environ. Res., 207 (2022) 112175, doi: 10.1016/j.envres.2021.112175.
[20] L. Ji, W.W. Chen, J. Bi, S. Zheng, Z. Xu, D. Zhu, P.J. Alvarez, Adsorption of tetracycline on single-walled and multi-walled carbon nanotubes as affected by aqueous solution chemistry, Environ. Toxicol. Chem., 29 (2010) 2713–2719.
[21] Y. Zhao, J. Geng, X. Wang, X. Gu, S. Gao, Adsorption of tetracycline onto goethite in the presence of metal cations and humic substances, J. Colloid Interface Sci., 361 (2011) 247–251.
[22] Ö. Hanay, B. Yıldız, S. Aslan, H. Hasar, Removal of tetracycline and oxytetracycline by microscale zerovalent iron and formation of transformation products, Environ. Sci. Pollut. Res., 21 (2014) 3774–3782.
[23] P.-H. Chang, Z. Li, T.-L. Yu, S. Munkhbayer, T.-H. Kuo, Y.-C. Hung, J.-S. Jean, K.-H. Lin, Sorptive removal of tetracycline from water by palygorskite, J. Hazard. Mater., 165 (2009) 148–155.
[24] Q. Shen, M.H. Xu, T. Wu, G.X. Pan, P.S. Tang, Adsorption behavior of tetracycline on carboxymethyl starch grafted magnetic bentonite, Chem. Pap., 76 (2022) 123–135.
[25] Y.Y. Liu, L.Q. Li, Z.S. Duan, Q.L. You, G.Y. Liao, D. Wang, Chitosan modified nitrogen- doped porous carbon composite as a highly-efficient adsorbent for phenolic pollutants removal, Colloids Surf., A, 610 (2021) 125728, doi: 10.1016/j.colsurfa.2020.125728.
[26] H. El Harmoudi, L. El Gaini, E. Daoudi, M. Rhazi, Y. Boughaleb, M.A. El Mhammedi, A. Migalska-Zalas, M. Bakasse, Removal of 2,4-D from aqueous solutions by adsorption processes using two biopolymers: chitin and chitosan and their optical properties, Opt. Mater., 36 (2014) 1471–1477.
[27] A.G.S. Prado, J.D. Torres, E.A. Faria, S.C.L. Dias, Comparative adsorption studies of indigo carmine dye on chitin and chitosan, J. Colloid Interface Sci., 277 (2004) 43–47.
[28] G. Pigatto, A. Lodi, E. Finocchio, M.S.A. Palma, A. Converti, Chitin as biosorbent for phenol removal from aqueous solution: equilibrium, kinetic and thermodynamic studies, Chem. Eng. Process. Process Intensif., 70 (2013) 131–139.
[29] H. Tang, W. Zhou, L. Zhang, Adsorption isotherms and kinetics studies of malachite green on chitin hydrogels, J. Hazard. Mater., 209–210 (2012) 218–225.
[30] X. Wang, B. Xing, Importance of structural makeup of biopolymers for organic contaminant sorption, Environ. Sci. Technol., 41 (2007) 3559–3565.
[31] M. Rinaudo, Chitin and chitosan: properties and applications, Prog. Polym. Sci., 31 (2006) 603–632.
[32] R. Dolphen, N. Sakkayawong, P. Thiravetyan, W. Nakbanpote, Adsorption of Reactive Red 141 from wastewater onto modified chitin, J. Hazard. Mater., 145 (2007) 250–255.
[33] S. Żółtowska-Aksamitowska, P. Bartczak, J. Zembrzuska, T. Jesionowski, Removal of hazardous non-steroidal anti-inflammatory drugs from aqueous solutions by biosorbent based on chitin and lignin, Sci. Total Environ., 612 (2018) 1223–1233.
[34] I. Langmuir, The adsorption of gases on plane surfaces of glass, mica, and platinum, J. Am. Chem. Soc., 40 (1918) 1361–1403.
[35] S. Cengiz, F. Tanrikulu, S. Aksu, An alternative source of adsorbent for the removal of dyes from textile waters: *Posidonia Oceanica* (L.), Chem. Eng. J., 189–190 (2012) 32–40.
[36] H. Freundlich, Over adsorption in solution, J. Phys. Chem., 57 (1906) 385–470.
[37] C. Muthukumaran, V.M. Sivakumar, M. Thirumarimurugan, Adsorption isotherms and kinetic studies of crystal violet dye removal from aqueous solution using surfactant modified magnetic nanoadsorbent, J. Taiwan Inst. Chem. Eng., 63 (2016) 354–362.
[38] M.M. Dubinin, E.D. Zaverina, L.V. Radushkevich, Sorption and structure of active carbons. I. Adsorption of organic vapors, Zh. Fiz. Khim., 21 (1947) 1351–1362.
[39] S. Lagergren, Zur Theorie Der Sogenannten Adsorption Geloster Stoffe, Kungliga Svenska Vetenskapsakademiens Handlingar Band, 24 (1898) 1–39.
[40] Y.S. Ho, G. McKay, Pseudo-second-order model for sorption processes, Process Biochem., 34 (1999) 451–465.
[41] W.J. Weber, J.C. Morris, Kinetics of adsorption on carbon from solution, J. Sanit. Eng. Div. Am. Soc. Civ. Eng., 89 (1963) 31–59.
[42] M.E. Mahmoud, G.M. Nabil, N.M. El-Mallah, H.I. Bassiouny, S. Kumar, T.M. Abdel-Fattah, Kinetics, isotherm, and thermodynamic studies of the adsorption of Reactive Red 195 A dye from water by modified Switchgrass Biochar adsorbent, J. Ind. Eng. Chem., 37 (2016) 156–167.
[43] J.M. Smith, H.C. Van Ness, Introduction to Chemical Engineering Thermodynamics, 4th ed., McGraw-Hill, Singapore, 1987.
[44] A.M. Adel, Z.H. Abd El-Wahab, A.A. Ibrahim, M.T. Al-Shemy, Characterization of microcrystalline cellulose prepared from lignocellulosic materials. Part II: physicochemical properties, Carbohydr. Polym., 83 (2011) 676–687.
[45] S. Dhananasekaran, R. Palanivel, S. Pappu, Adsorption of Methylene Blue, Bromophenol Blue, and Coomassie Brilliant Blue by α-chitin nanoparticles, J. Adv. Res., 7 (2016) 113–124.
[46] S. Erdogan, M. Kaya, High similarity in physicochemical properties of chitin and chitosan from nymphs and adults of a grasshopper, Int. J. Biol. Macromol., 89 (2016) 118–126.
[47] Z. Zheng, B. Zhao, Y. Guo, Y. Guo, T. Pak, G. Li, Preparation of mesoporous batatas biochar via soft-template method for high efficiency removal of tetracycline, Sci. Total Environ., 787 (2021) 147397, doi: 10.1016/j.scitotenv.2021.147397.
[48] Z. Aksu, I.A. Isoglu, Use of dried sugar beet pulp for binary biosorption of Gemazol Turquoise Blue-G reactive dye and copper(II) ions: equilibrium modeling, Chem. Eng. J., 127 (2007) 177–188.
[49] M.H. Marzbali, M. Esmaieli, H. Abolghasemi, M.H. Marzbalic, Tetracycline adsorption by H_3PO_4-activated carbon produced from apricot nut shells: a batch study, Process Saf. Environ. Prot., 102 (2016) 700–709.
[50] M. Gonzalez-Davila, F.J. Millero, The adsorption of copper to chitin in seawater, Geochim. Cosmochim. Acta, 54 (1990) 761–768.
[51] S.A. Khedr, M.A. Shouman, A.A. Attia, Adsorption studies on the removal of cationic dye from shrimp shell using chitin, Biointerface Res. Appl. Chem., 3 (2012) 507–519.
[52] P. Szymczyk, U. Filipkowska, T. Jóźwiak, M. Kuczajowska-Zadrożna, Phosphate removal from aqueous solutions by chitin and chitosan in flakes, Prog. Chem. Appl. Chitin Der., 21 (2016) 192–202.
[53] M. Abbas, M. Trari, Kinetic, equilibrium and thermodynamic study on the removal of Congo red from aqueous solutions by adsorption onto apricot stone, Process Saf. Environ. Prot., 98 (2015) 424–436.
[54] A.Y. Dursun, O. Tepe, Removal of Chemazol Reactive Red 195 from aqueous solution by dehydrated beet pulp carbon, J. Hazard. Mater., 194 (2011) 303–311.
[55] Z. Aksu, A.I. Tatlı, O. Tunc, A comparative adsorption/biosorption study of Acid Blue 161: effect of temperature on equilibrium and kinetic parameters, Chem. Eng. J., 142 (2008) 23–39.
[56] H. Peng, W. Xiong, Z. Yang, J. Cao, M. Jia, Y. Xiang, Q. Hu, Z. Xu, Facile fabrication of three-dimensional hierarchical porous ZIF-L/gelatin aerogel: highly efficient adsorbent with excellent recyclability towards antibiotics, Chem. Eng. J., 426 (2021) 130798, doi: 10.1016/j.cej.2021.130798.
[57] D.M.R.E.A. Dissanayake, W.M.K.E.H. Wijesinghe, S.S. Iqbal, N. Priyantha, M.C.M. Iqbal, Isotherm and kinetic study on Ni(II) and Pb(II) biosorption by the fern *Asplenium nidus* L, Ecol. Eng., 88 (2016) 237–241.
[58] M. Tanyol, V. Yonten, V. Demir, Removal of phosphate from aqueous solutions by chemical- and thermal-modified bentonite clay, Water Air Soil Pollut., 226 (2015) 269, doi: 10.1007/s11270-015-2538-8.
[59] A. Kadous, M. Amine, A new sorbent for uranium extraction: ethylenediamino-tris(methylenephosphonic) acid grafted on polystyrene resin, J. Radioanal. Nucl. Chem., 284 (2010) 431–438.
[60] J. Pan, X. Bai, Y. Li, B. Yang, P. Yang, F. Yu, J. Ma, HKUST-1 derived carbon adsorbents for tetracycline removal with

excellent adsorption performance, Environ. Res., 205 (2022) 112425, doi: 10.1016/j.envres.2021.112425.
[61] A. Kumar, C. Patra, S. Kumar, S. Narayanasamy, Effect of magnetization on the adsorptive removal of an emerging contaminant ciprofloxacin by magnetic acid activated carbon, Environ. Res., 206 (2022) 11260, doi: 10.1016/j.envres.2021.112604.
[62] A. Einbu, K.M. Vårum, Characterization of chitin and its hydrolysis to GlcNAc and GlcN, Biomacromolecules, 9 (2008) 1870–1875.
[63] N. Rokhati, T.D. Kusworo, H. Susanto, I.N. Widiasa, N. Aryanti, A. Adhiartha, Y. Fahni, N.A. Hamada, Preparation of glucosamine by acid hydrolysis of chitin under microwave irradiation, AIP Conf. Proc., 2197 (2020) 070001, doi: 10.1063/1.5140934.